Fractal patterns, cluster dynamics, and elastic properties of magnetorheological suspensions

J. L. Carrillo, F. Donado, and M. E. Mendoza

Instituto de Física de la Universidad Autónoma de Puebla, Apartado Postal J-48, Puebla 72570, Puebla, México

We study pattern formation and the aggregation processes in magnetorheological suspensions in the presence of a static magnetic field, and some of their associated physical properties. In particular, we analyze the elastic modes as a function of the intensity of the applied field and for several particle concentrations. We observe that the clusters formed in these systems have multifractal characteristics, which are the result of three well defined stages of the aggregation process. In these stages three generations of clusters are produced sequentially. The structure of the suspension can be well characterized by its mass fractal dimensions and the mass radial distribution. The size distribution of the second-generation clusters written in terms of their mass fractal dimension allows us to calculate the sound speed of the longitudinal modes in the large wavelength regime. This multifractal analysis applied to several kinds of aggregates reveals that the occurrence of at least three stages of aggregation is a common feature to several physical aggregation processes.

I. INTRODUCTION

During the last few years rheological suspensions of dipolar particles have been a subject of great interest for basic as well as for applied research. The many body interactions among the particles, which cause the complex structure of the suspension, and the link between this structure and the macroscopic physical properties of the system, still present several unanswered fundamental questions [1]. Upon the application of an external magnetic field, magnetorheological suspensions (MRS's) suffer a quasireversible transition from a liquid system to almost a solid body in times of the order of a few milliseconds. Obviously, this change in the mechanical properties of the dispersion is due to the structure formed by the particles. The understanding of these phenomena requires of some insights in the knowledge about the behavior of systems of interacting dipolar particles. In the presence of an external field, the MRS's acquire a fibrous structure, which sometimes has been described as bunches of chains formed by piledup particles [2]. However, it has been theoretically discussed that for dipolar particles this situation is possible only as a limiting law case, under the conditions of low particle concentration and intense applied field [3]. However, experimental results indicate that in more general conditions, the acquired cluster structure in the dispersion is in fact much more complex.

It has been found in many classes of condensed matter systems that clusters produced by an aggregation process exhibit a structure where a statistical short range order exists. However, at larger scales there appears a symmetry dilation, which confers a fractal feature to the structure [4]. Moreover, there exists evidence that also some complex fluids, in particular the magnetorheological suspensions in the presence of a magnetic field, arrange locally in hcc or in tetragonal structures [2], although, in some of those complex systems at larger scales, fractal characteristics of the clusters have been observed [2,5,6]. It has been shown that there exists a relationship between the hierarchical nature of the structure and the aggregation processes which generate it [5]. The internal structure of the clusters is determined by several factors such as the intensity of the interaction among the particles, the interaction with external fields, the thermal energy, the liquid viscosity, the polarizability, the shape, the mean size, and the main symmetries of the suspended particles. Some models have been proposed to describe the structure of rheological fluids [2,7]. In most of these models, however, a simplification in the calculation of the rheological response and the physical properties of the suspension is introduced, namely, it is assumed that, under the application of a magnetic field, the particles in the system form an ordered structure. Although, it has been observed that a complex structure is formed even for small concentrations, about $\phi = 0.01$ in volume fraction [3,8,9]. We have observed that clustering in ordered structures is only the first one, of at least three stages, of the aggregation processes which build up the structure in a MRS.

In this work we discuss our observations of pattern formation and its relationship with some of the physical properties of the MRS, particularly with the elastic properties. First, we briefly describe the preparation and characterization of the iron oxide particles which we use for the rheological suspensions. Then, we discuss our observations by optical microscopy of complex pattern formation in the MRS induced by the applied field. The observed patterns are characterized by means of their mass fractal dimension and the radial mass distribution. On this basis, we discuss how the intensity of the applied magnetic field and other external parameters can change the cluster structure. By using an effective media approach we calculate the elastic properties of the suspension. Our attention is focused on the propagation of elastic perturbations in these systems. The sound speed in the suspension under different physical conditions is studied. Finally, we discuss the application of our multifractal analysis to other condensed matter aggregates. We found that the occurrence of at least three stages of aggregation is a common feature to the aggregation process in several physical systems.

II. AGGREGATION PATTERNS

For the preparation of the MRS we synthesize iron oxide particles (Fe_3O_4) of prismatic morphology by means of a
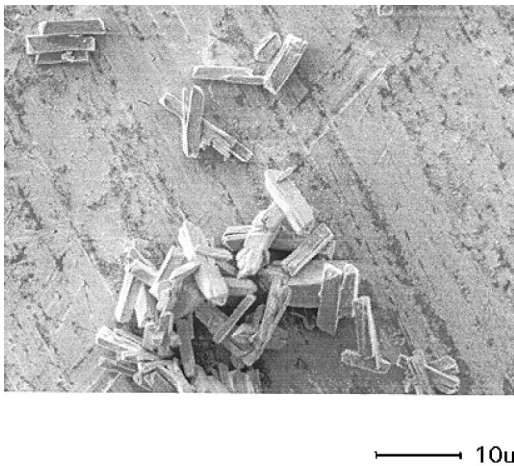
FIG. 1. Iron oxide particles with prismatic habit used in the preparation of the MRS.

coprecipitation procedure. These particles are obtained as precipitates in a small volume reaction of aqueous solutions of ammonium oxalate, iron (III) nitrate, and iron (II) chloride, followed by thermal decomposition. We used x-ray diffraction to determine the obtained phases. The difractograms show the presence of magnetite and some traces of maghemite. Figure 1, shows a scanning electron microscopy (SEM) photograph of the particles. Note the unusual prismatic habit of the particles. They are homogenous in form and with a sharp distribution of sizes about 10 μm [10]. To prepare the MRS, these particles were dispersed in silicone oil. To be able to observe the structure by optical microscopy, we use low particle concentrations, less than 0.1 in volume fraction.

Using cover glass we prepare square cells, 15-mm wide and 1-mm thick, to contain the dispersion. To observe the pattern formation, one of these cells is set on the stage of the optical microscope and the magnetic field is applied using electromagnets. We use the light transmitted mode for our observations.

The process of pattern formation is filmed with a digital camera. We observe the whole process, beginning some time before applying the field. In absence of the applied field the particles are homogeneously dispersed in the silicone oil and we can observe the individual particles moving through the liquid. The processes of aggregation when the field is turned on are as follows: the magnetization induced in the particles produces an attraction among nearest neighbors, which leads to the aggregation of particles. This clustering process driven by the dipolar interaction occurs throughout the system, producing relatively small first-generation clusters, whose structure is often crystallinelike arranged. In this latter aspect our observations agree with the results of some reported numerical simulations which indicate that the structure of the system is statistically and locally ordered [2].

After this relatively rapid aggregation stage there follows the aggregation of the first-generation clusters. Now, due to the larger average diameter of the clusters, viscosity effects become more important. Also, as a consequence of the finite size of the particles and the noncompact structure of the clus-

ters, the dipolar interaction intensity and range do not scale with cluster size. Hence, due to the relatively short range of the dipolar potential, the mechanical interactions among clusters, and the viscosity effects, the order of the structure is lost in this aggregation stage. More properly described, there occurs a symmetry dilation in the structure of the second-generation clusters formed in this stage. We have observed a third aggregation stage. In this stage, second-generation clusters aggregate and rearrange to form the final fibrous structure of the dispersion. One expects that this sequence of stages or patterns of aggregation would be correlated with the change in the rheological behavior of the system, where the first and second aggregation stages would contribute to these changes. Note that these patterns and their relation with the interactions driving the aggregation processes are as expected in the time evolution of an out of equilibrium system, namely, the more intense the interaction, the shorter the time in which its effect is felt.

Since the first-generation clusters are the building blocks for the second- and the third-generation clusters, this implies that, locally, throughout the fibrous structure, there exist statistically ordered small arrays of particles. The average range of this order is as long as the mean size of the first-generation clusters.

The existence of this statistical local order has been usually interpreted as the formation of chains or bunches of chains along the system. We have observed in MRS of prismatic, but also of spheroidal magnetic, particles that the clusters of the different generations exhibit some asymmetry in their shape; they are usually longer in the direction of the applied field. This has been interpreted as the incomplete aggregation of chains [11]. There has been some discussion regarding the cause of this asymmetry. It has been argued that in the aggregation process, the hydrodynamic interactions cause anisotropic diffusion of the particles along and normal to their axes [12]. Due to the presence of the static magnetic field the aggregation process driven by dipolar interactions is essentially anisotropic for any shape of the particles. For no very low particle concentration ($\phi > 0.01$), not only the hydrodynamic interactions might contribute to the loss of order in the structure, but also some other phenomena of entropic nature. For instance, in the aggregation process the particles or clusters, in its respective stage of aggregation, obstruct each other denying an ordered arrangement.

To specify and quantify the features of this pattern formation, we measure the cluster mass fractal dimension D, defined by the well known power law $m \sim r^D$, where m is the mass contained in a circle of radius r. To measure the fractal dimension of the complex structure generated in the system by the application of a magnetic field, we proceed as follows. From the sequences of digital video we take some pictures of different regions of the structure in its final configuration. Then we make an image treatment to obtain a more contrasted image, so as to define only one plane of the structure. Then, we draw a number of equally separated concentric circles, starting with a circle of diameter of the order of the mean size of the particles, up to circles as large as the observation field allows, the separation between contiguous circles being also of the order of the particle mean size. Provided
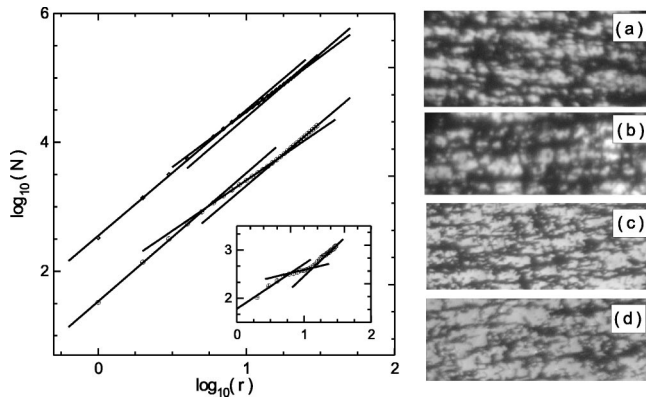
FIG. 2. $\log_{10}N$ versus $\log_{10}r$ for structures formed in a magnetorheological system, for two particle volume fractions, lower curve $\phi=0.04$ and upper $\phi=0.06$. The values of r are expressed in terms of the particle mean size σ. Inset: $\log_{10}(N_i-N_{i-1})$ vs $\log_{10}r_i$ corresponding to the lower curve. Right side, micrographs of the cluster structure: (a) 700 G and (b) 400 G, both of them with $\phi=0.06$. (c) 500 G and (d) 400 G, both with $\phi=0.04$.

FIG. 3. The average size of the first-generation r_{g_1} and the second-generation clusters r_{g_2} in a magnetorheological system as a function of the applied field for two values of the volume fraction.

that the number of pixels is proportional to the mass in a given element of area, we count the number of pixels contained in the circles. We repeat this procedure taking different sites, arbitrarily chosen, as centers of the set of circles. For all the sites we obtain relatively close values for the corresponding number of pixels. However, in order to avoid the effects of small local inhomogeneities and, mainly, to statistically capture the trends of the global structure, we average the number of pixels obtained for the corresponding circles for all the sites in the structure. Empirically we have found that a set of 30 circles and 10 sites is enough to obtain no significant differences. In this way, we determine the mass fractal dimension, characteristic of the stages of aggregation by which the hierarchical structure of the system is formed.

Figure 2 shows the behavior of the mass fractal dimension for two particle concentrations, 0.04 and 0.06 in volume fraction, and for different intensities of applied field. There, we have depicted the graph of $\log_{10}N_i$ versus $\log_{10}r_i$, where N_i is the number of pixels contained in the circle of radius r_i. Note that for both cases the corresponding graph has three clearly distinguishable portions, associated to the three aggregation stages mentioned above.

Each portion has a linear behavior and has been fitted by a straight line using the least squares method, considering a statistical error given by the dispersion of the $\log_{10}N_i$ values for the respective r_i. The lower curve corresponds to a MRS of Fe_3O_4 particles dispersed in silicone oil with a volume fraction of $\phi=0.04$ with an applied magnetic field of 700 G; the upper one to a volume fraction of $\phi=0.06$. We have shifted the figures vertically to make the comparison clear. Note the close similarity between both curves, showing straight portions revealing clearly similar aggregation processes yielding the hierarchical patterning. The changes of the aggregation stages are more evident in the radial scaling of the mass density. The inset shows the behavior of the mass radial distribution $\log_{10}(N_i-N_{i-1})$ as a function of $\log_{10}r_i$, corresponding to the lower curve. On the right side of the
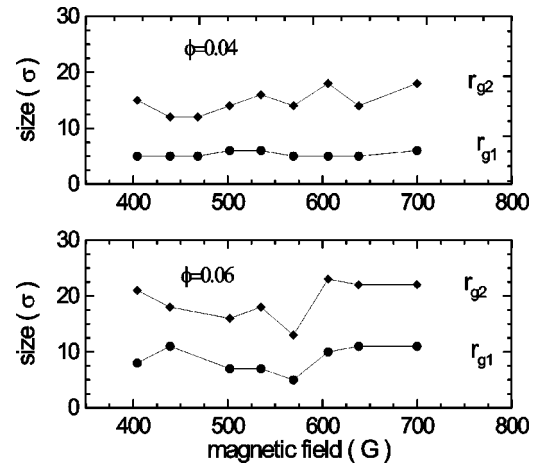
figure appear pictures of agglomerates in a MRS for different conditions: (a) 700 G and (b) 400 G, both with a volume fraction $\phi=0.06$. (c) 500 G and (d) 400 G, both with $\phi=0.04$. The elongated structures observed in the pictures are the second-generation clusters. We have noted that the average length of these substructures has some dependence on the intensity of the applied field.

Because the aggregation processes are driven essentially by dipolar interactions, with the corresponding scaling for the different generations, one may expect that the average size of the clusters, and their average formation time, should depend on the volume fraction as well as on the applied field intensity.

Figure 3 shows the average size r_{g_1} of the first-generation clusters as a function of the applied magnetic field for two values of the volume fraction, as well as the corresponding situation for the second-generation clusters. From Figs. 2 and 3 one may infer that the volume fraction and the applied field intensity are important parameters which determine the ranges in which the aggregation processes are predominantly individual particle aggregation, and this in turn determines the average size of the statistically ordered first-generation structures, yielding a change in the average size of the second-generation clusters. However, for the third-generation structures the relative changes in the average size are much smaller. We have extended the measurements to 55 circles with the same separation as before and the trend observed for radii larger than r_{g_2} remains the same. This characterization of the different stages of the pattern formation clearly exhibits the multifractal nature of the structure and allows us to determine the average size of the substructures in the system. Obviously, the interaction among these substructures must determine some of the physical properties of the system.

We have also studied how the cluster geometrical characteristics are affected by external variables such as the temperature, the field intensity, and the particle concentration. Due to the micrometric size of the particles, the thermal randomization of the magnetization can be neglected. However, we observed that the speed of the aggregation processes is

influenced by the temperature, rather than by the shape or size of the clusters. This effect is more noticeable at low temperatures, in the range where the viscosity of silicone oil increases.

By using videomicroscopy a direct measurement of the times characteristic of the aggregation stages is rather difficult, except for very low particle concentration ($\phi < 0.01$). Nevertheless, even in this range of low particle concentration it is possible to observe that the characteristic times decrease with the increasing of the particle concentration. This could be understood by considering that the characteristic times are mainly determined by the intensity of the applied field, the volume fraction, and the viscosity of the liquid, because these three factors must strongly determine the intensity of the interaction driving the aggregation at the different stages, namely, $\tau_i \sim 1/V_i$, V_i being the interaction potential magnitude and the subindex i labels the aggregation stages. It follows that, for the first stage, where the dipole interaction produces the particle aggregation, one may expect a dependence $\tau_1 \sim r^3$, r being the distance between two particles. Then, because of the dependence of r on the volume fraction we are led to $\tau_i \sim \phi^{-1}$. On the other hand, one may expect that the viscosity effects become important as the characteristic diameter of the moving clusters increases. Considering Stokes approximation, it is easily seen that the characteristic times of the aggregation at the different stages must be proportional to the effective diameter of the aggregating elements, namely, $\tau_i \sim \sigma_i$, with σ_i being σ, r_{g1}, and r_{g2}, respectively. This allows us to obtain the following simple relation among the characteristic times

$$\frac{\tau_1}{\tau_2} \sim \frac{\sigma}{r_{g1}}, \quad \frac{\tau_1}{\tau_3} \sim \frac{\sigma}{r_{g2}}. \tag{1}$$

The values of r_{g1} and r_{g2} can be obtained from the multifractal analysis as shown in Figs. 2 and 3. Measured times for the formation of the structure in MRS of about 100 ms have been reported [13]. Assuming a volume fraction such that the formation of the third-generation clusters takes this characteristic time, one obtains by using the above relations, the following estimated characteristic times for the formation of the first- and second-generation clusters: $\tau_1 \approx 6$ ms and $\tau_2 \approx 35$ ms.

The kinetics of the aggregation processes of dipolar magnetic particles has been studied both theoretically [12] and experimentally [14,15], under several schemes and techniques. In particular the time scaling regimes in the aggregation of magnetic dipolar particles have been studied by means of scattering dichroism. It is worth noting that also in those dynamical conditions, different time scaling regimes are detected [15].

In the low particle concentration condition, second-generation clusters are substructures whose shape is clearly distinguishable in the global structure of the dispersion. We search for the effect of the intensity of the applied field on the fractal properties of the second-generation clusters. In Fig. 4 we show our measurements of the mass fractal dimension of three dimensional second-generation clusters D_{2g} as a function of the applied field. The mass fractal dimension for
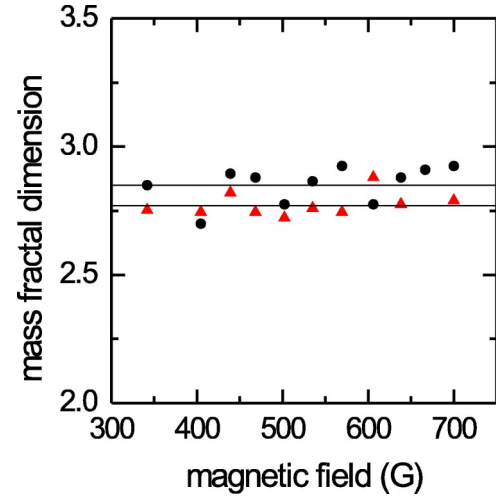

FIG. 4. The three-dimensional fractal dimension of the second-generation clusters as a function of the applied field, for two values of the volume fraction: triangles, $\phi = 0.04$ and dots, $\phi = 0.06$.

the three-dimensional clusters can be estimated from the measured values of the two-dimensional ones, by means of the relation $D_3 = 3/2D_2$. It is an easy task to prove that this relation is exact for Cantor-like fractal structures.

Note that for this range of relatively small magnitudes of applied field, the fractal dimension of the second-generation clusters does not exhibit a definite dependence. However, it is clear that the mass dimension does depend on the particle concentration.

The above results lead us to assume that, given a particle concentration, D_{2g} depends only on the fundamental symmetries of the particles and on their magnetic properties. Since these particles have soft magnetic properties, in this range of applied field, the polarizability does not change drastically. This is why the mass fractal dimension does not show a strong dependence on the magnitude of the applied field.

III. ELASTIC PROPERTIES

Presently, the study of classical waves propagating in complex condensed matter systems is a subject of great relevance. Despite the fact that this has been a topic widely studied for long time, the novel techniques and the capabilities of finely controlling the characteristics of the complex media have made it possible to find new surprising and interesting results and a vast amount of data [16].

In the calculation of the elastic properties of the fibrous structure acquired by the rheological dispersion in the presence of an external magnetic field, the complex structure is often treated as an arrangement of chains, or, in the opposite extreme, as homogeneous dispersion. However, these crude models of the structure predict quantitatively wrong elastic properties. We wish to explore how the multifractal cluster nature of the structure can be incorporated into the calculations.

According to Fig. 3 the typical size of the second-generation clusters is about 10 or 20 times the particle mean size. Consequently, one expects that these clusters might
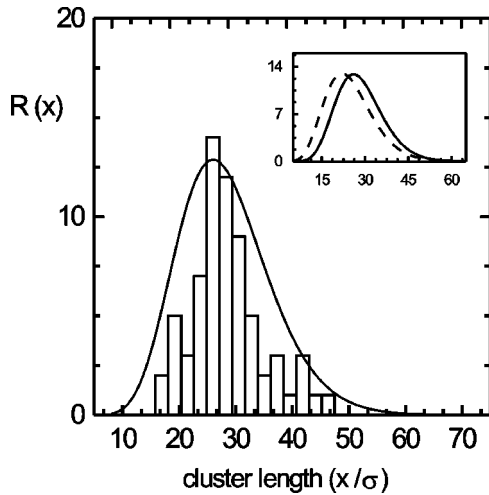
FIG. 5. The measured size distribution of the second-generation clusters for a volume fraction $\phi = 0.06$. Inset: Comparison of the size distribution for two different intensities of applied field, 350 G (left) and 500 G (right).

have an important role in determining some of the elastic properties of the rheological dispersions. To investigate this situation, we measure directly from the photographs the size of the second-generation clusters and construct a size frequency distribution; then, we compare it with the results obtained from the analysis of the mass fractal behavior, as appears in Fig. 3.

Figure 5 shows the measured cluster longitudinal-size distribution for an applied magnetic field of 500 G and for a volume fraction $\phi = 0.06$. In the same sample we made the measurement of the cluster size distribution for another value of the applied field (350 G), previously redispersing the suspension. From the comparison of the envelops, which appears in the inset, one sees that, as expected, the most frequent cluster size increases with the intensity of the applied field. Note that the agreement of these measurements with the second-generation cluster size predicted by the multifractal analysis, Fig. 3, is quite good. However, we think that the estimation of the average size via the fractal dimension is a more reliable procedure, since, in the direct measurement of the cluster size in the photographs, one introduces some error with the choice of the ending part of the clusters, for those portions of them that touch or overlap with other clusters.

It has been shown that in systems with complex correlations, the expected distribution of the relevant physical quantities has the form $f(x) = Cx^p e^{p(q)}$, p and q being real numbers [17]. The following phenomenological expression, which fits well the measured second-generation cluster size distribution, can be obtained by using some heuristic arguments:

$$R(x) = \alpha(\phi) x^{D\lambda} e^{-D/\lambda}. \qquad (2)$$

Here $\lambda = Bm/kT$ is the ratio of the magnetic to the thermal energy, m being the particle magnetization, B the local magnetic field, which can be estimated by means of a Weiss-like mean field approximation, T is an effective temperature which incorporates the viscosity effects, and D is the mass

fractal dimension. Since D can be measured and λ estimated, there are no free or fitting parameters in this expression. It is worth remarking that the most frequent cluster size is $\Sigma = \lambda^2$, and the quantity $\alpha(\phi)$ is a constant which can be calculated by means of a normalization condition [18].

We have found that for low to moderate intensities of applied magnetic field, 500–5000 G, the above expression fits well the frequency size distribution of the three-dimensional second-generation clusters formed in dispersions of iron oxide particles, with a size distribution in the range 10–40 μm [18]. In fact, the envelops of the measured distributions, which appear in Fig. 5, were calculated using this expression. Furthermore, we have found that Eq. (2) describes accurately the cluster size distribution in MRS prepared with iron particles and also, under similar conditions of particle concentration and moderate intensities of applied electric field, in electrorheological dispersions [19]. In this sense, Eq. (2) reveals a general trend in the aggregation processes and in the pattern formation in dispersions of dipolar particles.

We search now the role played by the clusters of different generations, in the elastic properties of a rheological dispersion in the presence of a magnetic field.

Sound speed

The elastic properties of a MRS are determined by the interactions among the particles and among the clusters of all generations. The elastic response of the system will depend on the wavelength of the elastic perturbation propagating through the dispersion. We focus our attention in the long wavelength elastic perturbations by which sound propagates in complex liquids. For these elastic perturbations, with wavelength much larger than the particle mean size, some approximations are commonly used. Provided that dissipative effects can be neglected, one may adopt one of the simplest effective media approximations to calculate the sound speed. We assume that the system behaves as a continuous medium with effective elastic modulus and density; then, the sound speed can be evaluated by means of the expression [20]

$$v = \left(\frac{\beta}{\rho} \right)^{1/2}, \qquad (3)$$

where the effective density is given by

$$\rho = \phi \rho_s + (1 - \phi) \rho_f \qquad (4)$$

and the effective elastic modulus is

$$\beta = \beta_s^{-1} \phi + \beta_f^{-1} (1 - \phi), \qquad (5)$$

where the subindex labels the solid and liquid phases.

For dispersions of smaller particles, in the regime of wavelength much larger than the particle mean size, only one elastic longitudinal mode is expected to propagate. Also, because the fluid does not support any shear, transversal modes cannot exist in these systems. However, still in this regime,

one could expect that the intensity of the applied field has some influence on the elastic longitudinal mode in MRS.

The surprising and intriguing observation of two longitudinal elastic modes propagating in a magnetorheological slurry in the long wavelength regime [21] has been reported. One of them, called the first mode, was associated with the expected sound propagation through channels in the structure, where essentially the oil is the medium which supports the elastic perturbation. This is because the propagation speed of this mode was measured to be close to the sound speed in the pure liquid.

The unexpected second mode was observed to be slower than the first one and appears only in the presence of an applied magnetic field. It was associated with the propagation of sound through the fibrous structure formed by the particles. The propagation speed of both modes was observed to depend on the intensity of the applied magnetic field [21].

The simple effective media approximation, Eqs. (3)–(5), was used to describe the first one of the observed modes. It provides an accurate description of the experimental results for the sound speed, as a function of the particle volume fraction and as a function of the applied field intensity [21], however, it fails to describe correctly the second mode propagation. We now proceed to incorporate the multifractal nature of the MRS structure in the study of the propagation of elastic modes.

IV. RESULTS AND DISCUSSION

To calculate the sound speed for the two observed longitudinal modes we assume that the first mode propagates through almost clear oil channels. Considering only the average value of the density, we obtain a better agreement with the measured results in comparison to those obtained by using the effective values for the density and the elastic modulus [21]. For weak magnetic fields, the oil channels contain a dilute dispersion of iron particles, which affects only the inertial properties of the composite medium, namely, the value of the density, but it does not not modify the elastic properties. This would be more suitable for high magnetic fields, because as we have discussed above, cluster size increases with the magnetic energy, and then, more particles stick to the clusters, fewer of them remaining in the oil channels. The second mode was associated with the propagation of an elastic mode through the fibrous structure of the suspension. To calculate the sound speed of this second mode, we use the same effective media approximation but model the system as a suspension of effective macroparticles (second-generation clusters) dispersed in the oil. We need then to evaluate the effective density and elastic modulus of the second-generation clusters. This can be easily done by considering the mass scaling and the second-generation cluster mean size, and the following procedure to evaluate the elastic constant of the clusters in terms of a first-neighbors magnetic interaction. The dipolar force between two magnetic spheres whose centers are separated by a distance r is given by
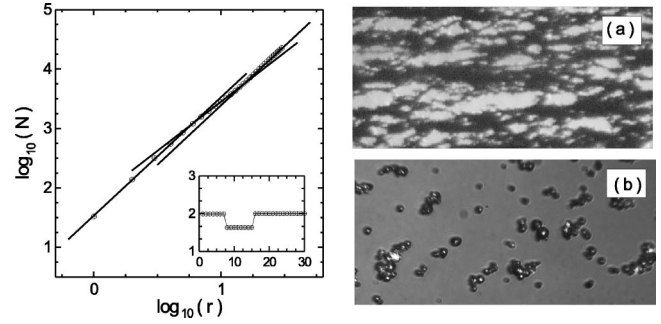

FIG. 6. $\log_{10}N$ vs $\log_{10}r$ for structures formed in MRS prepared with iron spheroidal particles dispersed in glycerine, $\phi=0.06$. The values of r are expressed in terms of the particle mean size σ. Inset: The mass fractal dimension as a function of r. Right side: Micrographs of the cluster structure (a) and particles (b).

$$F=-\frac{3\mu_0}{2\pi}\frac{m_s^2}{r^4},\qquad(6)$$

where μ_0 is the magnetic permeability and m_s is the magnetic polarization of the spheres.

Dividing this expression by the cross section area of the structure formed by the second-generation clusters, the longitudinal stress is obtained. Then, taking the derivative with respect to the longitudinal strain, namely, $r(\partial/\partial r)$, one obtains the elastic modulus $\beta=\frac{2}{3}\mu_0M^2$, M being the cluster magnetization.

We have conducted experiments with iron spheroidal particles dispersed in glycerine, our multifractal analysis reports very similar results to those obtained for iron oxide prismatic particles dispersed in silicone oil, namely, the mean cluster size of each generation has practically the same value. Also the scaling behavior is closely the same. These characteristics are shown in Fig. 6. In the right side of this figure there is a picture of the structure of a MRS prepared with iron particles, with average size about 20 μm, dispersed in glycerine, with a volume fraction $\phi=0.06$, and applied field of 650 G. There appears also a micrograph of individual particles. The mass scaling behavior is shown in the left side with a graph of $\log_{10}N_i$ versus $\log_{10}r_i$. Comparing with Fig. 2, one observes the very close agreement, even quantitatively, between both MR systems. The mass fractal dimension as a function of r appears in the inset, showing clearly the different mass scaling regions corresponding to the aggregation stages.

In Fig. 7(a) we show our results for the sound speed for both modes as a function of the volume fraction of the suspended particles. The dots and the dashed line are the experimental results for the first and second modes, respectively [21]. The continuous lines are the results obtained by the effective media approximation, Eqs. (2)–(5), averaging only the density for the first mode, and considering second-generation clusters as macroparticles dispersed in the oil for the second one. The scale for this second mode appears at the right side. The arrow indicates the particle volume fraction used for the measurements of the sound speed in terms of the applied field [21].
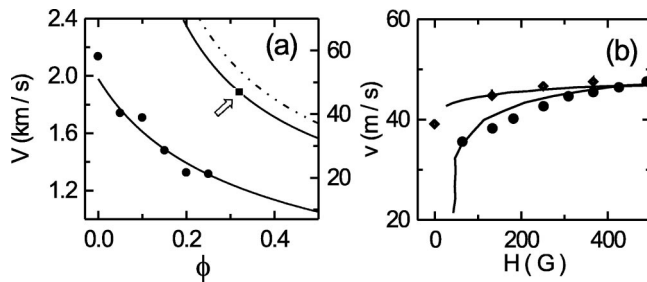
FIG. 7. (a) The sound speed of the first and second modes as a function of the particle volume fraction. The scale for the second mode appears at the right side. (b) The sound speed for the second mode as a function of the field intensity. Dots and squares are the measured values for increasing and decreasing intensities, respectively

Figure 7(b) shows our results (continuous line) for the sound speed as a function of the intensity of the magnetic field. Dots and squares are the measured values [21] for increasing and decreasing intensities, respectively.

V. SIMILARITIES WITH OTHER AGGREGATES

Using the procedure discussed in Sec. II, we have analyzed some other cluster structures formed by aggregation processes, after considering the proper changes in the scales for the analysis. We have found in all of them a behavior of the fractal dimension analogous to that of the MRS discussed with relation to Fig. 2. In Fig. 8 we show a comparison of the fractal dimension for clusters of (a) an aggregate of coagulated blood, (b) a tetraethoxisilane (TEOS) gel, and (c) a cluster numerically generated by diffusion limited aggregation (DLA).

Except for case (c), we note a qualitatively analogous behavior to that found for the MRS aggregates. Again, there are three different stages clearly differentiated. We conclude, then, that this procedure of analyzing the fractal dimension of the final structure in complex systems allows us to statistically define the stages of the aggregation processes associated to the predominant interactions, as well as the average size of the clusters of the respective generations. Some related results had been obtained for aggregates of smaller particles [4,5,22].

The cluster generated by DLA exhibits qualitatively important differences. One of them is that the whole structure is accurately described by a single fractal dimension. One may conclude that DLA, in general, is not able to describe real aggregation processes, because DLA does not account prop-
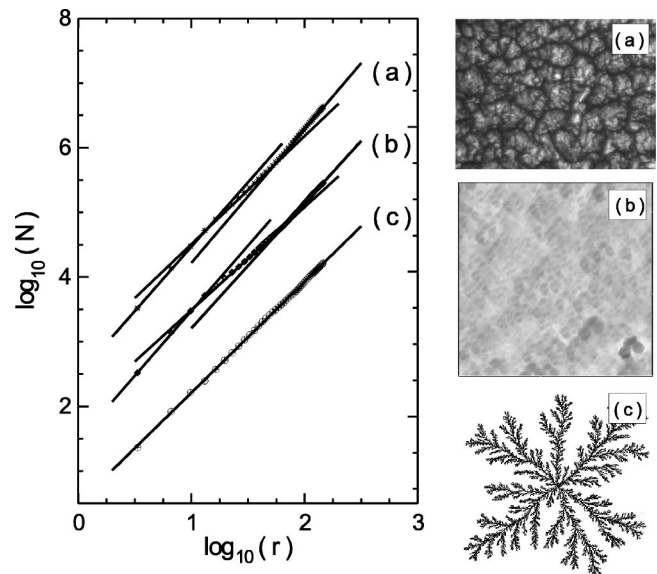

FIG. 8. For different systems formed by aggregation processes the behavior of the fractal dimension exhibits similar characteristics. Curve (a) a coagulated blood cluster, (b) a TEOS gel cluster, and (c) a cluster obtained numerically by DLA.

erly for the scaling of the different variables and also because it does not incorporate information, of entropic nature, for instance, which could be determinant factors, at least for clusters formed by weakly interacting particles.

In the case of aged TEOS gels and making a more detailed multifractal analysis, we have observed a possible fourth stage suggested by the trend of its fractal dimension. In this later stage the patterning indicates an aggregation process which yields a structure whose mass fractal dimension tends to reach its maximum value. We have analyzed several kinds of aged gels and we obtain this trend invariably. We suggest that this behavior could be associated to the slow events of aggregation in the latest polymerization steps. Analogous conclusions for the scaling behavior in gels have been obtained from studies by small angle x-ray scattering SAXS, performed on silica aerogels [23] and from dynamical analysis by static light scattering and dynamic light scattering, of the aging processes on colloidal gels [24].

[1] A. Kawai *et al.* in *Proceedings of the Eighth International Conference on Electro-Rheological Fluids and Magneto-Rheological Suspensions*, edited by G. Bossis (World Scientific, Singapore, 2002); J. DeVicente *et al.*, *ibid.*; W.H. Lee *et al.*, *ibid.*

[2] G.L. Gulley and R. Tao, Phys. Rev. E **56**, 4328 (1997).

[3] Y. Levin, J. Phys.: Condens. Matter **14**, 2303 (2002).

[4] D.A. Weitz and M. Oliveria, Phys. Rev. Lett. **52**, 1433 (1984).

[5] D.A. Weitz, Phys. Rev. Lett. **54**, 1416 (1985).

[6] L.J. Huang and W.M. Lau, J. Phys.: Condens. Matter **5**, 7087 (1993).

[7] L.C. Davis, Appl. Phys. Lett. **73**, 680 (1993); J. Appl. Phys. **72**,

1334 (1994).

[8] F. Donado, M.E. Mendoza, and J.L. Carrillo, Physica A **295**, 81 (2001).

[9] J. Fan, X. Zhao, X. Gao, and C. Cao, J. Phys. D **35**, 88 (2002).

[10] M.E. Mendoza, F. Donado, R. Silva, M.A. Pérez, and J.L. Carrillo (unpublished).

[11] G. Helgesen, A.T. Skjeltorp, P.M. Mors, R. Botet, and R. Jullien, Phys. Rev. Lett. **61**, 1736 (1988).

[12] M. Carmen Miguel and R. Pastor-Satorras, Phys. Rev. E **59**, 826 (1999).

[13] See, for instance, S. Cutillas, and J. Liu, in *Proceedings of the Seventh International Conference*, edited by R. Tao (World Scientific, Singapore, 1999), p. 260.

[14] S. Melle, G.G. Fuller, and M.A. Rubio, Phys. Rev. E **61**, 4111 (2000).

[15] S. Melle, M.A. Rubio, and G.G. Fuller, Phys. Rev. Lett. **87**, 115501 (2001).

[16] C.H. Liu and S.R. Nagel, Phys. Rev. Lett. **68**, 2301 (1992); Phys. Rev. B **48**, 15 646 (1993); L. Ye, J. Liu, P. Sheng, and D.A. Weitz, Phys. Rev. E **48**, 2805 (1993).

[17] See, for instance, F. Haake, G. Lenz, P. Seba, J. Stein, H.J. Stockmann, and K. Zyczkowski, Phys. Rev. A **44**, R6161 (1991).

[18] F. Donado, J.L. Carrillo, and M.E. Mendoza, J. Phys.: Condens. Matter **14**, 2153 (2002).

[19] F. Donado, M.E. Mendoza, V. Dossetti, E. López-Cruz, and J.L. Carrillo, Ferroelectrics **270**, 93 (2002).

[20] P. Sheng, in *Homogenization and Effective Moduli of Materials and Media*, edited by J.L. Ericksen, D. Kinderlehrer, R. Khon, and J.-L. Lions (Springer-Verlag, New York, 1986); Z. Hazhin, J. Appl. Mech. **29**, 143 (1962).

[21] Y. Nahmad-Molinari, C.A. Arancibia-Bulnes, and J.C. Ruiz-Suárez, Phys. Rev. Lett. **82**, 727 (1999).

[22] D.W. Schaefer, J.E. Martin, P. Wiltzius, and D.S. Cannell, Phys. Rev. Lett. **52**, 2371 (1984).

[23] D.W. Schaefer and K.D. Keefer, Phys. Rev. Lett. **56**, 2199 (1986).

[24] L. Cipelletti, S. Manley, R.C. Ball, and D.A. Weitz, Phys. Rev. Lett. **84**, 2275 (2000).